Superseded by NASA TN D-745

Copy 196
RM L56B07

NACA RM L56B07

CLASSIFICATION CHANGED TO: Unclassified
Per: Pub 12-14
rep 1

NACA

APR 27 1956

RESEARCH MEMORANDUM

MEASUREMENTS OF AERODYNAMIC HEAT TRANSFER AND BOUNDARY-LAYER TRANSITION ON A 10° CONE IN FREE FLIGHT AT SUPERSONIC MACH NUMBERS UP TO 5.9

By Charles B. Rumsey and Dorothy B. Lee

Langley Aeronautical Laboratory
Langley Field, Va.

CASE FILE COPY

CLASSIFIED DOCUMENT

This material contains information affecting the National Defense of the United States within the meaning of the espionage laws, Title 18, U.S.C., Secs. 793 and 794, the transmission or revelation of which in any manner to an unauthorized person is prohibited by law.

NATIONAL ADVISORY COMMITTEE FOR AERONAUTICS

WASHINGTON

April 26, 1956

NATIONAL ADVISORY COMMITTEE FOR AERONAUTICS

RESEARCH MEMORANDUM

MEASUREMENTS OF AERODYNAMIC HEAT TRANSFER AND BOUNDARY-LAYER TRANSITION ON A 10° CONE IN FREE FLIGHT AT SUPERSONIC MACH NUMBERS UP TO 5.9

By Charles B. Rumsey and Dorothy B. Lee

SUMMARY

Measurements of aerodynamic heat transfer have been made at six stations on the 40-inch-long 10° total-angle conical nose of a rocket-propelled model which was flight tested at Mach numbers up to 5.9. Data are presented for a range of local Mach number just outside the boundary layer on the cone from 1.57 to 5.50, and a range of local Reynolds number from 6.6×10^6 to 55.2×10^6 based on length from the nose tip.

At Mach numbers up to 4, measurements of laminar, transitional, and turbulent heat-transfer coefficients were obtained. In general, the measured laminar heat-transfer coefficients expressed as Stanton number agree well with theory for laminar heat transfer on a cone. The measured turbulent heat-transfer coefficients expressed as Stanton number agree reasonably well with turbulent theory for heat transfer on a cone with Reynolds number based either on length from the nose tip or length from the transition point.

During the last part of the flight test when the Mach number was above approximately 4, the measured heat-transfer coefficients were consistently about midway between the theoretical laminar and turbulent heat-transfer values all along the nose.

Experimental transition Reynolds numbers varied from less than 8.5×10^6 to 19.4×10^6. At a relatively constant ratio of wall temperature to local static temperature near 1.2, the transition Reynolds number increased from 9.2×10^6 to 19.4×10^6 as Mach number increased from 1.57 to 3.38. At a relatively constant Mach number near 3.7, the transition Reynolds number decreased about 30 percent as the ratio of wall temperature minus adiabatic wall temperature to stagnation temperature changed from -0.35 to -0.25.

During the flight, local Mach number and the ratio of wall temperature to local static temperature simultaneously reached values well within the region for infinite laminar stability predicted by two-dimensional disturbance theory. The transition Reynolds number increased to a maximum value of 19.4×10^6 as the test conditions probed into the theoretical stability region.

INTRODUCTION

The Pilotless Aircraft Research Division is conducting a program to measure the aerodynamic heat transfer and boundary-layer transition Reynolds numbers on bodies in free flight at high Mach numbers. References 1 and 2 reported heat-transfer data obtained from skin-temperature measurements at single stations on 10° total-angle conical noses at flight Mach numbers up to approximately 4. In the present investigation, measurements of skin temperature were made at six stations on a 40-inch-long 10° total-angle conical nose in order to obtain the variation in heat transfer along the nose and to determine the location of boundary-layer transition. Data were obtained up to a maximum flight Mach number of 5.9 with a corresponding local Mach number on the cone just outside the boundary layer of 5.5. The maximum local Reynolds number at the most rearward temperature measurement station, based on length from the nose tip, was 55.2×10^6. The model was expected to reach a Mach number of 7, but a structural failure ended the test at a time approximately two-thirds through the burning period of the last propulsion stage.

The flight test was conducted at the Langley Pilotless Aircraft Research Station at Wallops Island, Va.

SYMBOLS

A	area, sq ft
C_H	Stanton number, $\frac{h}{gC_p\rho_V V_V}$
C_p	specific heat of air at constant pressure, Btu/lb-$^\circ$F
C_w	specific heat of wall material, Btu/lb-$^\circ$F
g	gravitational constant, ft/sec-sec

h	local aerodynamic heat-transfer coefficient, Btu/sec-sq ft-^{o}F
J	mechanical equivalent of heat, ft-lb/Btu
k	thermal conductivity of air, Btu-ft/sec-^{o}F-sq ft
k_w	thermal conductivity of wall material, Btu-ft/sec-^{o}F-sq ft
M	Mach number
Pr	Prandtl number, $\frac{C_p \mu}{k}$
Q	quantity of heat, Btu
R	Reynolds number, $\frac{\rho V x}{\mu}$
R.F.	recovery factor, $\frac{T_{aw} - T_v}{T_{so} - T_v}$
T	temperature, ^{o}R except as noted
t	time, sec
V	velocity, ft/sec
x	distance along nose surface from tip, ft
σ	Stefan-Boltzman constant, 0.4806×10^{-12} Btu/sq ft-sec-$^{o}R^{4}$
ϵ	emissivity
ρ	density of air, slug/cu ft
ρ_w	density of wall material, lb/cu ft
τ	thickness of wall material, ft
μ	absolute viscosity of air, slugs/ft-sec

Subscripts:

aw	adiabatic wall
o	undisturbed free stream ahead of model
so	stagnation

v local condition just outside boundary layer

w wall

tr condition at beginning of transition

MODEL AND TESTS

Model Configuration

The general configuration of the model is shown by the photograph, figure 1(a), and pertinent dimensions are given in the drawing, figure 1(b). The body was a cone cylinder 150 inches long, of overall fineness ratio 21.4. The total angle of the conical nose was 10°, which made the nose fineness ratio 5.71. The nose was constructed of Inconel skin approximately 0.030 inch thick, except for the tip which was made of stainless steel, hollowed out as shown in figure 1(b) and welded to the skin at station 6. The exterior surface of the entire nose was highly polished. The surface roughness as measured by a Physicists Research Company Profilometer was 3 to 4 microinches rms over the forward 20 inches and about 5 microinches rms over the back 20 inches of the nose. The cylindrical body which housed the sustainer rocket motor was rolled from sheet steel. The stabilizing fins were steel and were welded to the body at the base.

Model Instrumentation

Six thermocouples were embedded in the Inconel skin of the conical nose along an element at points 10, 14, 19, 24, 30, and 37 inches from the nose tip as shown in figure 1(b). The thermocouples were made of no. 30 chromel alumel wire. The junction between the wires consisted of a bead about 0.01 inch in diameter, formed by fusing the wires together using the mercury bath technique. Care was taken that the wires were not in contact except within the bead. The beads were fitted into holes drilled through the Inconel skin at the proper stations, with the thermocouple leads inside the nose. The holes were then welded closed with Inconel welding rod and the exterior surface was smoothed and polished. The cold junctions of the thermocouples were potted in paraplex inside a brass block of sufficient mass that no change in cold junction temperature would occur during the relatively short time of the test. The cold junction temperature was measured just prior to launching by a resistance-type temperature pickup also potted inside the brass block. A check of telemetered skin temperature was made just prior to launching by measuring the temperature at station 30 with a thermocouple taped to the exterior surface of the skin.

During flight, three standard voltages and the outputs of the six thermocouples were commutated and transmitted on a single telemeter channel. The commutation rate and the electronic system were such that each thermocouple voltage was transmitted 14 times per second, and each standard voltage was transmitted 7 times per second. The three standard voltages, supplied by a mercury cell and a voltage divider network, were chosen equivalent to the lowest temperature, the midrange temperature, and the highest temperature that the skin thermocouples were expected to reach. Commutation and transmission of these known voltages along with the voltage readings of the skin thermocouples provided an "in-flight" check calibration of the thermocouple telemeter and recording system.

Measurements of thrust acceleration and drag deceleration were also telemetered during flight. The instrumentation was carried in the nose section of the model and was protected from the high temperatures reached by the skin during flight by a radiation shield. The shield consisted of a frustrum of a cone extending from station $25\frac{1}{2}$ to station 40, closed at the front end, and spaced about $\frac{1}{4}$ inch inside the exterior skin. The shield was formed from 0.03-inch-thick Inconel, was highly polished, and was attached to the telemeter supports so as not to touch the exterior skin at any point.

Propulsion and Test Technique

The model was launched at an elevation angle of 70°. The three-stage propulsion system consisted of two M5 JATO boosters in tandem and an ABL Deacon sustainer motor. Figure 1(c) shows the model and boosters on the launcher. The first booster accelerated the combination to Mach number 1.4 and drag separated at burnout. The second-stage booster and the model, which were held together by a locking device, coasted upwards for a predetermined time until the second-stage booster ignited and accelerated the model and booster to a Mach number of 4.0. Chamber pressure of the firing booster released the locking device, which allowed the booster to drag separate at its burnout. After another predetermined coast period, the sustainer motor ignited and accelerated the model until a structural failure occurred at a Mach number of 5.9. The lengths of the coast periods were chosen in an attempt to obtain the maximum possible Mach number without exceeding allowable skin temperatures.

Velocity data were obtained by means of CW Doppler radar until a time shortly after ignition of the sustainer rocket. Integration of the telemetered thrust acceleration extended the velocity data to the time of model failure. Altitude and flight-path data were measured by

an NACA modified SCR 584 tracking radar. A marked change in the distance-time relation of the SCR 584 data at the time the telemeter record ended indicated that a structural failure had occurred. Atmospheric and wind conditions were measured by means of radiosondes launched near the time of flight and tracked by an AN/GMD-1A Rawin set.

Figure 2(a) shows time histories of the flight Mach number and the skin temperatures measured at the six stations on the nose cone. Time histories of altitude and free-stream Reynolds number per foot are shown in figure 2(b).

Data Reduction

The time rate of change of heat within the skin at a given location on the conical nose can be written

$$\frac{dQ}{dt} = \rho_w C_w \tau A \frac{dT_w}{dt} = hA(T_{aw} - T_w) - A\sigma\epsilon T_w^4 + Ak_w\tau\left[\frac{\partial^2 T_w}{\partial x^2} + \frac{1}{x}\frac{\partial T_w}{\partial x}\right] \quad (1)$$

The first term on the right-hand side represents the aerodynamic heating, the second term represents the heat radiated externally from the skin, and the third term represents the effect of heat conduction along the skin.

This statement of the heat balance neglects heat absorbed by the skin from solar radiation and heat radiated by the skin to the inner radiation shield. Estimates show that each of these factors is negligible (less than 1 percent of the aerodynamic heat transfer) at the test conditions for which heat-transfer data are reduced; further, their effects on the determination of heat-transfer coefficient are compensative.

Computed values of the term representing conduction along the skin for a time during the flight when the temperature gradients along the skin were large showed that the effect of conduction on the determination of aerodynamic heat-transfer coefficients was less than 0.2 percent at any measurement station, and the term was therefore disregarded.

Eliminating the conduction term, the expression for the aerodynamic heat-transfer coefficient h is then

$$h = \frac{\rho_w C_w \tau \frac{dT_w}{dt} + \sigma\epsilon T_w^4}{T_{aw} - T_w} \quad (2)$$

Experimental values of h at each measurement station were determined for several times during the test by using the measured skin temperatures and their time rates of change in equation (2). Other parameters required in equation (2) were obtained as follows.

The skin thickness τ at each of the measurement stations was measured, and ρ_w, the density of Inconel, was known. The variation of C_w, the specific heat of Inconel, is given in reference 1 for the temperature range 30° F to 930° F. The Stephan-Boltzman constant σ was known. A constant value of emissivity ϵ of 0.3 was used since tests performed by the National Bureau of Standards under a contract for the National Advisory Committee for Aeronautics, and as yet unpublished, show that the emissivity of unoxidized Inconel varies only slightly from 0.3 over the range of temperatures (75° F to 952° F) measured in the present test. It may be noted that the radiation term, $\sigma\epsilon T_w^4$, (see eq. (2)) comprised less than 20 percent of the heat-transfer coefficient for all cases, and less than 10 percent of C_H in 90 percent of the data. The remaining quantity needed in equation (2), T_{aw}, was computed from the relation

$$T_{aw} = R.F.(T_{so} - T_v) + T_v \tag{3}$$

where R.F. was determined from the usual turbulent relation R.F. = $Pr^{1/3}$ with Pr evaluated at wall temperature. Values of C_H of laminar magnitude were recomputed using the laminar relation for recovery factor, R.F. = $Pr^{1/2}$, to determine T_{aw}. Local static temperature T_v was obtained from the conical flow tables, reference 3 (with cone angle and free-stream conditions of Mach number and temperature known), and stagnation temperature T_{so} was computed from the energy equation

$$\frac{V^2}{2Jg} = \int_{T_o}^{T_{so}} C_p dT \tag{4}$$

which takes into account the variation of the specific heat of air with temperature. Values of the integral in equation (4) were obtained from tables in reference 4.

Having determined the experimental value of h from equation (2), the corresponding values of Stanton number based on local conditions just outside the boundary layer were computed from

$$C_H = \frac{h}{gC_p\rho_v V_v} \tag{5}$$

with the specific heat of air taken at T_v and obtained from reference 5.

RESULTS AND DISCUSSION

Skin Temperature Time Histories

The measured skin temperature time histories are shown in figure 2, with the flight Mach number plotted against the same time scale. During the first 12.5 seconds of the test, the heating and cooling of the skin were not intense because the velocity was relatively low. After 12.5 seconds the aerodynamic heating increased and the skin temperature at all stations rose rapidly. The maximum rate of rise was about 400° F per second, and the temperature at station 19 had reached 952° F when the telemeter record ended at 21.8 seconds. The irregularities in the skin temperature curves for the two most forward stations are the result of alternation between laminar and turbulent boundary-layer flow. The character of the boundary layer and the location of transition can be determined more readily from the magnitude of the heat-transfer coefficients and will be discussed later.

Heat Transfer

Local heat-transfer coefficients in the form of Stanton number were reduced from the skin temperature measurements, as described under Data Reduction, for several different times during the high Mach number part of the flight from 12.5 seconds until the end of the test. Figures 3(a) to 3(f) show the values of C_H obtained at stations 10, 14, 19, 27, 30, and 37, respectively. The data for each station are plotted against time because Mach number, Reynolds number, and the ratio of wall temperature to local static temperature all vary simultaneously during the test, thus making it impossible to isolate their individual effects on C_H. The variations of these parameters, M_v, R_v (based on length from the nose tip to the measurement station) and the temperature ratio T_w/T_v, are shown for each station on the same time scale as the experimental values of C_H. The local Mach number is identical for each station but is repeated on each figure for convenience. For comparison with the experimental C_H data, theoretical values for laminar flow and for turbulent flow at the test conditions are shown for each measurement station. The theoretical laminar values were obtained from the flat-plate theory of reference 6, multiplied by $\sqrt{3}$ to convert to

conical values. The theoretical turbulent values were obtained from Van Driest's theory for heat transfer on a cone with turbulent boundary layer from the nose, reference 7.

In figure 3(a), the experimental values of C_H for station 10 show that the irregularities in the temperature time curve of figure 2 are the result of alternations between laminar and turbulent boundary layer at the station. During the periods of low heating rates which are apparent in the temperature time history from 12.5 to 12.8 seconds, and from 13.5 to 14.2 seconds, the Stanton numbers at station 10 were laminar and in good agreement with the theory. From 15.6 to 18.0 seconds when the temperature rose very slowly (see fig. 2), the experimental values of C_H are considerably less than those for laminar theory. The reason for this difference is not understood. At times prior to 19.0 seconds, the heat-transfer coefficients of turbulent magnitude in general agree well with the theory for turbulent flow from the nose tip. The somewhat low values at 13.0 and 13.2 seconds are probably the result of transitional rather than completely turbulent flow. The measurements at 14.8 and 15.0 seconds may be high as a result of a transition location shortly ahead of station 10, which would make the actual turbulent Reynolds number less than that based on length from the tip. From 18.4 to 19.0 seconds, the measurements are in agreement with the theory for turbulent flow from the nose tip. From time 19.0 seconds, which is just before the start of the final acceleration period, until the end of the test the experimental C_H values lie between the laminar and turbulent theories and decrease rapidly during the last 0.8 second of the test. Since R_V remained near 10×10^6 during this time, a transitional boundary layer at this station (station 10) would not seem unusual. However, as will be noted in the succeeding plots of figure 3, the C_H data for each of the six measurement stations followed the same trends after 19 seconds, and lie between laminar and turbulent theory even though R_V at station 37 became as high as 41×10^6. Furthermore, the values of C_H at a given time do not increase with distance along the nose as would be expected if transitional flow existed all along the nose. If the model were flying at an angle of attack, the local flow conditions used to reduce h to C_H would of course be in error. An estimation of the influence of angle of attack was made by reducing the measured values of h to C_H using values of $C_p\rho_V V_V$ for the down-wind side of the cone at 5° angle of attack and for the up-wind side of the cone at 10° angle of attack. Neither assumption brought the experimental data into appreciably better agreement with either laminar or turbulent theory, and for structural reasons, much larger angles of attack do not seem probable over the relatively long time period from about 19 to 21.8 seconds and for the Mach number range covered. Since errors in the flight data or in the temperature measurements would have to be excessive to account for the difference between the measured C_H and the turbulent theory, it must be assumed that some unknown

factor influenced the results from 19.0 seconds until 21.8 seconds when a structural failure ended the test.

Figure 3(b) shows the test conditions and C_H values for the second measurement station from the nose, station 14. The C_H data vary between laminar and turbulent magnitude in the sequence indicated by the temperature time history in figure 2. Prior to 19.0 seconds, the laminar and turbulent theories are reasonably accurate lower and upper limits of the experimental values of C_H. The data indicate that at several times transitional flow existed at this station. From 19.0 seconds until the end of the test, the C_H values at this station, as at station 10, lie between the laminar and turbulent theory, although, as noted previously, the distribution of C_H along the nose is not that which would be expected for transitional flow.

Figure 3(c) shows the time histories of C_H and test conditions for station 19. The experimental C_H values agree reasonably well with the turbulent theory from 12.5 seconds until 19.0 seconds. After 19.0 seconds the data fall between the laminar and turbulent theory as at the first two measurement stations.

Figures 3(d), (e), and (f) show the time histories for stations 24, 30, and 37, respectively. Prior to 19 seconds the data at each station agree fairly well with the turbulent theory, but after 19 seconds the data fall between the laminar and turbulent theories. Between 12.5 and 15 seconds, conditions of M_V, R_V, and T_W/T_V occurred at station 30 which are almost identical to conditions that occurred during the tests reported in references 1 and 2. Data at these conditions from the three tests are comparable, since the cone angles and construction of the noses were the same for all three models. Some of the data from references 1 and 2 are shown on figure 3(e), the time history plot for station 30. The present values are slightly lower than those of the other tests, but the agreement is fair.

Boundary-Layer Transition

The variation of heat transfer along the nose and the location of boundary-layer transition are best shown by plots of C_H values against nose length for specific times. Figure 4(a) shows distributions of experimental and theoretical C_H values along the nose for times 12.5, 13.5, and 14.7 seconds which are during an acceleration period with Mach number and Reynolds number increasing with time. The measured values of C_H were laminar at the two forward stations and turbulent at the four rearward stations at times 12.5 and 13.5 seconds, and turbulent

at all stations at 14.8 seconds. With the assumption that transition began at the most rearward station having a laminar heat-transfer coefficient, values of the local Reynolds number at the beginning of transition R_{tr} were 9.2×10^6, 14.8×10^6, and less than 14.9×10^6 at times 12.5, 13.5, and 14.8 seconds, respectively. The corresponding local Mach numbers were 1.57, 2.56, and 3.81.

When the location of transition is known as for times 12.5 and 13.5 seconds, theoretical turbulent C_H values can be determined using Reynolds numbers based on length from the transition point rather than length from the nose tip. These values are shown on the plots for 12.5 and 13.5 seconds by the curves labeled "R_V assumed 0 at transition point." At each of these times, the theory based on distance from the transition point is about 25 percent higher than the theory based on length from the nose tip for station 19, 5 inches behind the transition point, but is less than 10 percent higher for station 30, 16 inches behind the transition point. At 12.5 seconds the measurements are lower than either of the theoretical curves, and at 13.5 seconds they are in reasonable agreement with both.

From 14.8 to 19.5 seconds, Reynolds number was decreasing with time since the model was coasting upward with a small decrease in Mach number with time. Figure 4(b) shows C_H distributions for times 16.0, 18.0, and 19.0 seconds. At 16.0 seconds, the experimental C_H was laminar at the forward station, transitional at the second, and turbulent at the four rearward stations. At 18.0 seconds, C_H was laminar at the forward station and turbulent at the others, and at 19.0 seconds it was turbulent at all stations. Corresponding transition Reynolds numbers were 12.9×10^6 at $M_V = 3.72$, 10.0×10^6 at $M_V = 3.62$, and less than 9×10^6 at $M_V = 3.59$. At time 16.0 seconds, the turbulent measurements are in good agreement with the theory based on length from the transition point. At 18.0 seconds, the turbulent measurements are closer to the theory based on length from the nose tip, although their maximum disagreement with the theory based on length from transition is less than 15 percent.

It is interesting to note from figures 4(a) and 4(b) that there is good agreement between the experimental data and the laminar and turbulent theories which assume isothermal conditions along the nose, even though the actual surface temperature distributions (fig. 2(a)) were far from isothermal and were considerably different at different times.

From 19.6 seconds until the end of the test at 21.8 seconds, the local Mach number increased from 3.6 to 5.5 while the Reynolds number was nearly constant. The distributions of C_H for times 20.0, 21.0,

and 21.6 seconds are shown in figure 4(c). The data have essentially the same trend with nose length as either the laminar or turbulent theory, and in magnitude, fall approximately midway between the two. Whatever the condition of the boundary layer, it apparently was the same all along the instrumented part of the nose. While the cause of the apparent eccentricity is unknown as noted previously, the high Mach number range of the data (between about 4 and 5.5) makes them of particular interest, and the results are reported since further tests may indicate the reason for this particular magnitude and distribution of heat transfer.

Several transition Reynolds numbers in addition to those indicated in figure 4 can be determined from the time histories of measured C_H, figure 3. For example, figure 3(b) shows laminar C_H at station 14 at time 13.8 seconds while station 19 had a turbulent C_H at this time. (Although C_H at station 19 was not determined at exactly 13.8 seconds, the temperature time curve in fig. 2 and the C_H values of fig. 3(c) are assurance that the boundary layer at station 19 was turbulent at all times between 12.5 and 19 seconds.)

The transition Reynolds numbers obtained from the data for times 12.5 to 19 seconds are noted in figure 5 on a plot which shows the variation of the temperature ratio T_w/T_v with local Mach number for this time period. As the Mach number increased from 1.57 to 3.38, T_w/T_v remained approximately 1.2. Then, while the Mach number remained relatively constant near 3.7, T_w/T_v increased from 1.36 to 2.25.

The solid curve shows the variation of the ratio T_{aw}/T_v. In general, the transition Reynolds numbers are largest when the skin is coldest with respect to T_{aw}; that is, when the test values of T_w/T_v are furthest below the curve of T_{aw}/T_v. Other tests, for instance reference 8, have shown increasing transition Reynolds numbers with increasing values of $(T_{aw} - T_w)$ at a constant Mach number. The present data at Mach numbers near 3.7 are in agreement with this trend. The data from a Mach number of 1.57 to a Mach number of 3.38 also show increasing R_{tr} with increasing $(T_{aw} - T_w)$; however, the pure effect of changing Mach number may also be influencing the values of R_{tr}.

Conditions of M_v and T_w/T_v below the broken line are those for theoretically infinite stability of the laminar boundary layer for two-dimensional disturbances, as given by reference 9. As the Mach number increased to 3.38 and the test conditions probed deeply into this stability region a considerable increase in R_{tr} occurred, but the maximum value was 19.4×10^6.

Dunn and Lin (ref. 10) have recently extended the theory of reference 9. They indicate that for three-dimensional disturbances infinite stability is unattainable, although stability to very large Reynolds numbers ($\sim 10^{12}$) might be obtained at somewhat colder wall conditions than those for infinite stability according to the two-dimensional theory. Specifically, a temperature ratio of 1.474 would be required at a Mach number of 4. Although a test condition close to this was obtained ($T_w/T_v = 1.36$ at a Mach number of 3.75), the transition Reynolds number of 19.4×10^6 was not unusually high.

The transition Reynolds numbers measured during the period of essentially constant T_w/T_v are plotted against local Mach number in figure 6(a). The times to which the points correspond, and the station and its temperature ratio at the beginning of transition are noted on the figure. The transition Reynolds numbers increased from 9.2×10^6 to 19.4×10^6 as the Mach number increased from 1.57 to 3.38. As noted previously, the skin cooling term $T_{aw} - T_w$ was increasing simultaneously with Mach number and probably influenced the transition Reynolds numbers. During this part of the test, the beginning of transition was consistently at station 14 except between 13.0 and 13.2 seconds when for unknown reasons transition moved ahead of station 10 (see fig. 3(a), resulting in the low values of R_{tr} at Mach numbers of 2.05 and 2.25.

The transition Reynolds numbers that occurred while the Mach number was near 3.7 and T_w/T_v was increasing (see fig. 5) are shown in figure 6(b). Values of R_{tr} are plotted against the commonly used parameter $\frac{T_w - T_{aw}}{T_{so}}$, and the present data are shown by the symbols. The Mach number varied only from 3.81 to 3.60 as shown in the key. As the skin temperature parameter changed from -0.35 to -0.25 the transition Reynolds number decreased about 30 percent. This trend did not exist at temperature parameter values more negative than -0.35 because the boundary layer was turbulent at even the most forward station from 14.6 seconds until 15.2 seconds. (See fig. 3(a).) The curve in figure 6(b) represents wind-tunnel data from reference 8 for a $9\frac{1}{2}^\circ$ total-angle cone-cylinder body. The test Mach number was 3.12 with Reynolds number per foot varying from 8×10^6 to 2.25×10^6 as the temperature parameter varied toward zero. The Reynolds number per foot of the present data varied from 18×10^6 to 11×10^6 as the temperature parameter varied toward zero. The flight values of R_{tr} are roughly three times greater than the wind-tunnel data and show a somewhat stronger influence of skin cooling on R_{tr} between temperature parameter values of -0.2 to -0.35.

Calculated Skin Temperatures

Computations of skin temperature at station 10 and at station 37 were made for the flight conditions, using theoretical laminar and turbulent heat-transfer coefficients, respectively. The resultant temperature time histories are shown in figure 7 along with the temperatures measured at stations 10 and 37. Laminar flow at station 10 during the entire test would have resulted in considerably lower temperatures for that station. Turbulent theory (with Reynolds number based on length from the nose tip) gave a temperature time history for station 37 which is in very good agreement with the measurements.

CONCLUDING REMARKS

Measurements of aerodynamic heat transfer have been made at six stations on the 40-inch-long 10° total-angle conical nose of a rocket-propelled model which was flight tested at Mach numbers up to 5.9. Data are presented for a range of local Mach number just outside the boundary layer on the cone from 1.57 to 5.50, and a range of local Reynolds number based on length from the nose tip from 6.6×10^6 to 55.2×10^6.

At Mach numbers up to 4, measurements of laminar, transitional, and turbulent heat-transfer coefficients were obtained. In general, the measured laminar coefficients, in the form of Stanton number, agreed well with flat-plate laminar theory increased by the factor $\sqrt{3}$ to account for the conical nose shape. The measured turbulent coefficients expressed as Stanton number agreed reasonably well with turbulent theory for heat transfer on a cone with Reynolds number based either on length from the nose tip or on length from the transition point.

During the last part of the flight test when the Mach number was above approximately 4, the measured heat-transfer coefficients were consistently about midway between the theoretical laminar and turbulent values all along the nose.

Experimental values of Reynolds number at the beginning of transition varied from less than 8.5×10^6 to 19.4×10^6. At a relatively constant ratio of wall temperature to local static temperature near 1.2, the transition Reynolds number increased from 9.2×10^6 to 19.4×10^6 as Mach number increased from 1.57 to 3.38. At Mach numbers near 3.7, the transition Reynolds number decreased about 30 percent as the ratio of wall temperature minus adiabatic wall temperature to stagnation temperature changed from -0.35 to -0.25.

During the flight test, local Mach number and the ratio of wall temperature to local static temperature simultaneously reached values well within the region for infinite laminar stability predicted by two-dimensional disturbance theory. The transition Reynolds numbers increased to a maximum of 19.4×10^6 as the test conditions probed deeply into this theoretical stability region.

Langley Aeronautical Laboratory,
National Advisory Committee for Aeronautics,
Langley Field, Va., January 26, 1956.

REFERENCES

1. Rumsey, Charles B., Piland, Robert O., and Hopko, Russell N.: Aerodynamic-Heating Data Obtained From Free-Flight Tests Between Mach Numbers of 1 and 5. NACA RM L55A14a, 1955.

2. Rumsey, Charles B.: Free-Flight Measurements of Aerodynamic Heat Transfer to Mach Number 3.9 and of Drag to Mach Number 6.9 of a Fin-Stabilized Cone-Cylinder Configuration. NACA RM L55G28a, 1955.

3. Staff of the Computing Section, Center of Analysis (Under Direction of Zdeněk Kopol): Tables of Supersonic Flow Around Cones. Tech. Rep. No. 1, M.I.T., 1947.

4. Keenan, Joseph H., and Kaye, Joseph: Thermodynamic Properties of Air Including Polytropic Functions. John Wiley & Sons, Inc., 1945.

5. Woolley, Harold W.: Thermal Properties of Gases. Table 2.10, Nat. Bur. Standards, July 1949.

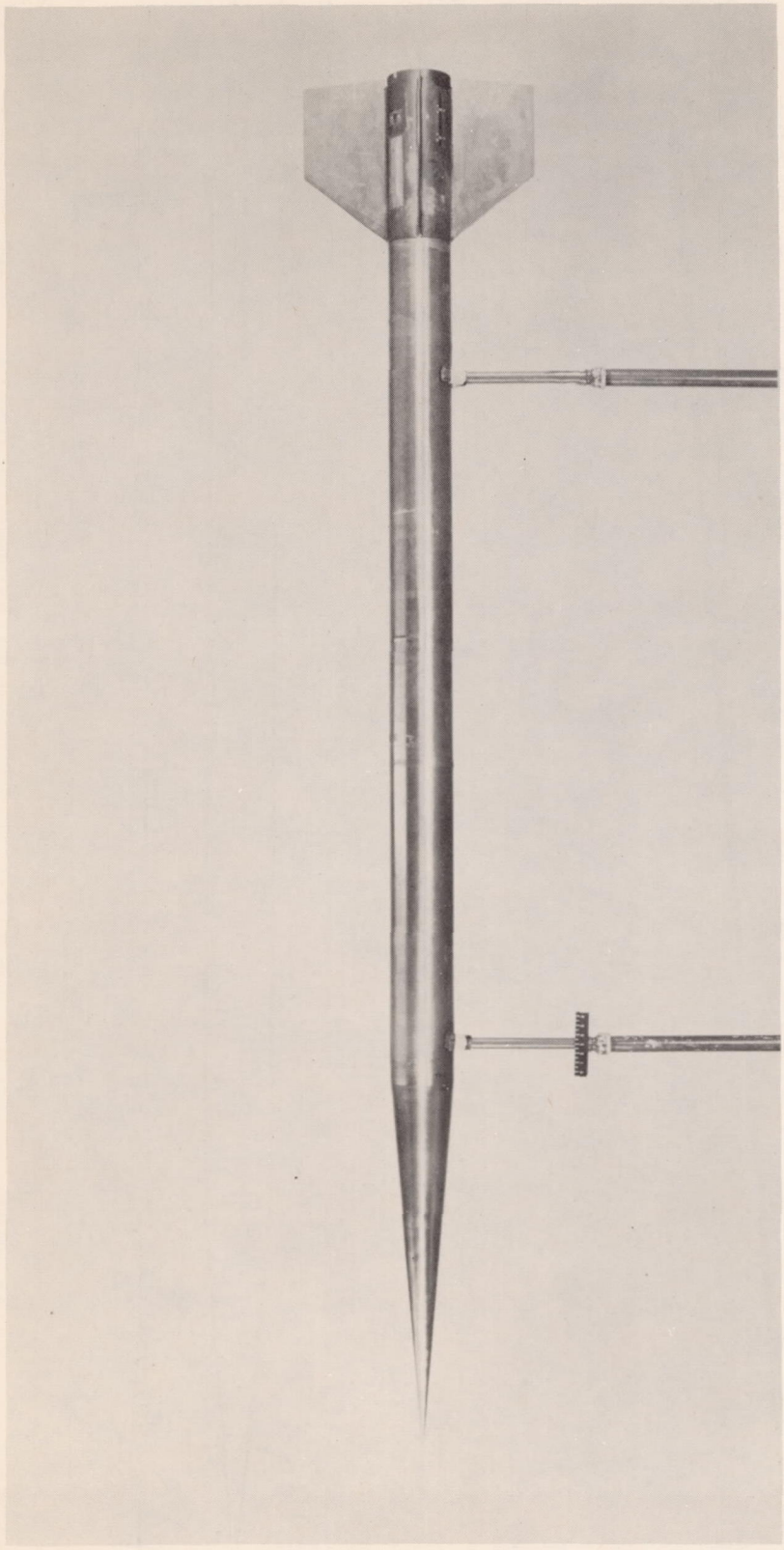
6. Van Driest, E. R.: Investigation of Laminar Boundary Layer in Compressible Fluids Using the Crocco Method. NACA TN 2597, 1952.

7. Van Driest, E. R.: Turbulent Boundary Layer on a Cone in a Supersonic Flow at Zero Angle of Attack. Jour. Aero. Sci., vol. 19, no. 1, Jan. 1952, pp. 55-57, 72.

8. Jack, John R., and Diaconis, N. S.: Variation of Boundary-Layer Transition With Heat Transfer on Two Bodies of Revolution at a Mach Number of 3.12. NACA TN 3562, 1955.

9. Van Driest, E. R.: Calculation of the Stability of the Laminar Boundary Layer in a Compressible Fluid on a Flat Plate With Heat Transfer. Jour. Aero. Sci., vol. 19, no. 12, Dec. 1952, pp. 801-812.

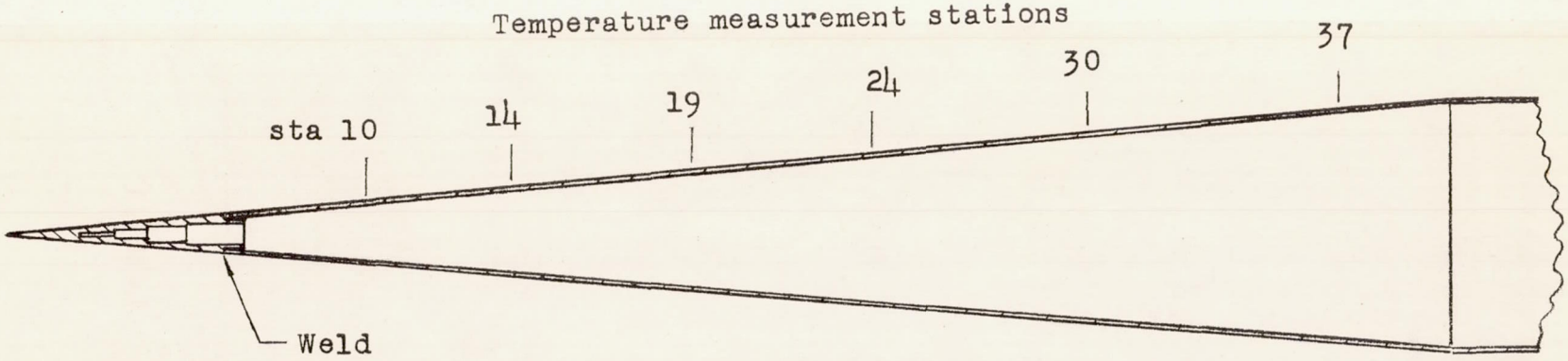
10. Dunn, D. W., and Lin, C. C.: On the Stability of the Laminar Boundary Layer in a Compressible Fluid. Jour. Aero. Sci., vol. 22, no. 7, July 1955, pp. 455-477.



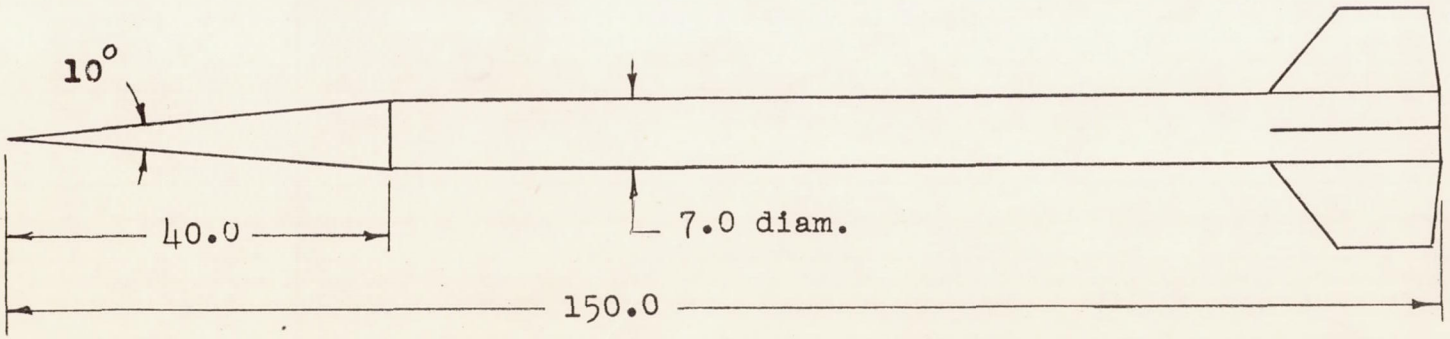
L-86090.1

(a) Photograph of model.

Figure 1.- Test configuration.

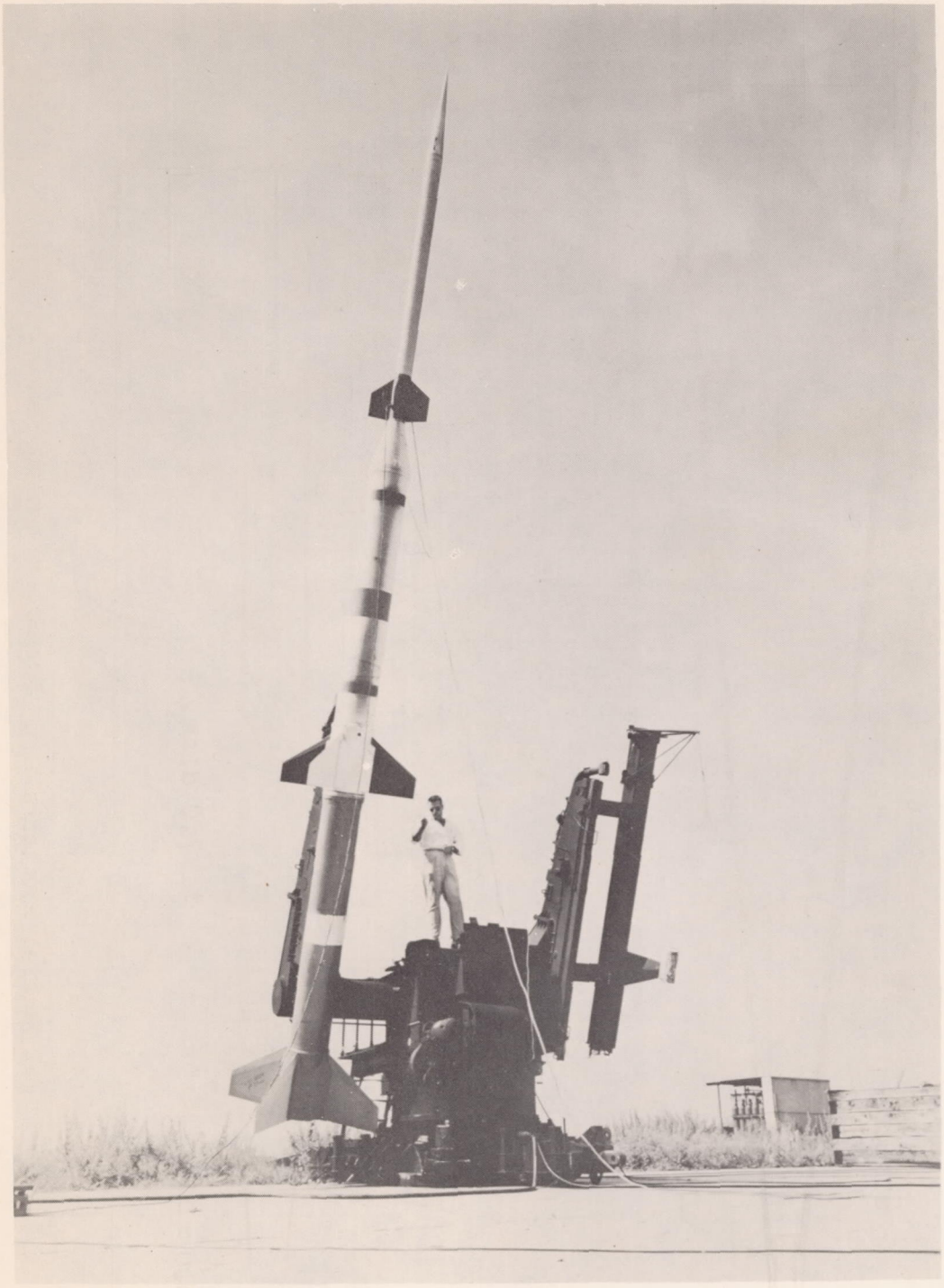


Nose detail



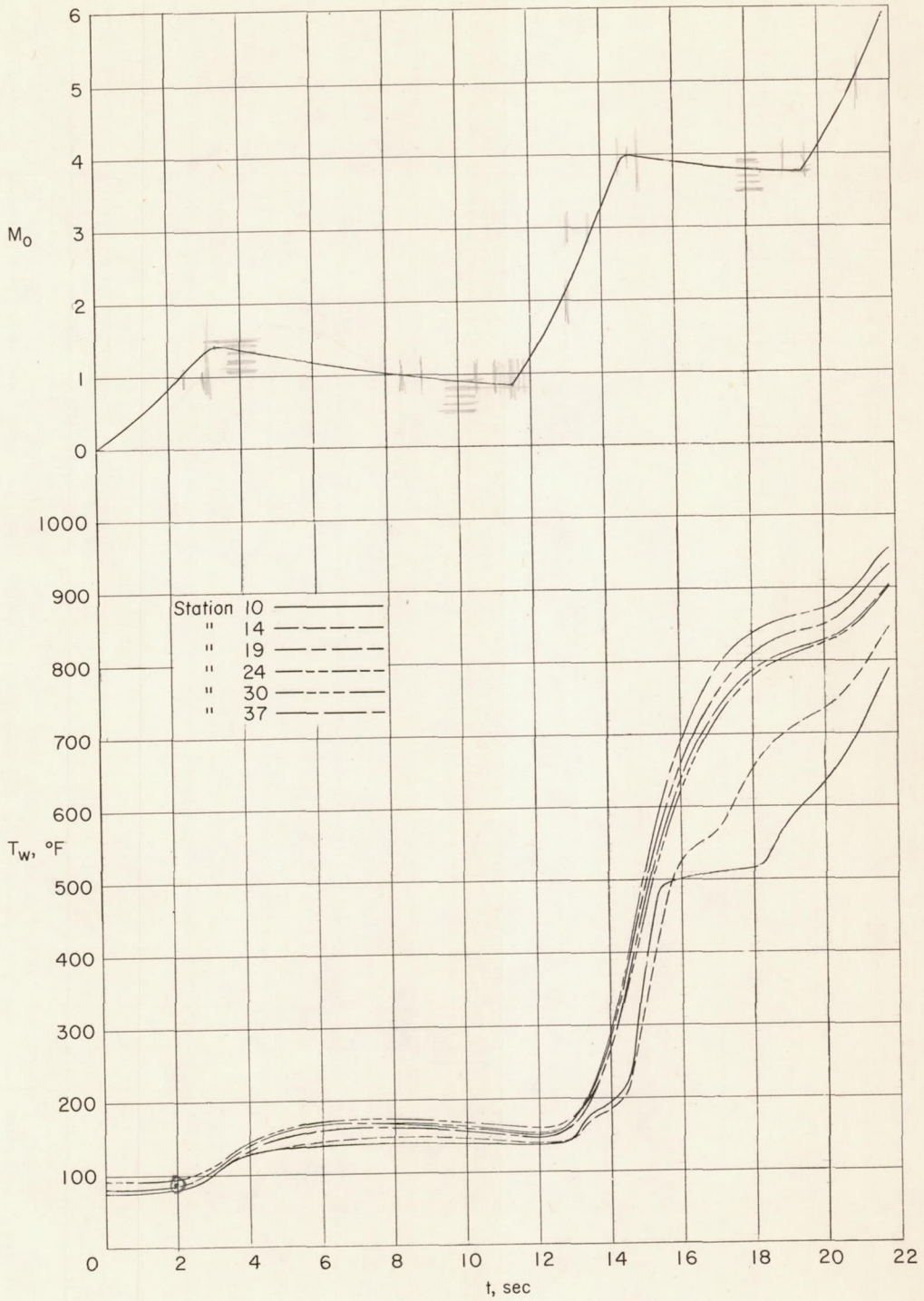
(b) General configuration. Dimensions are in inches.

Figure 1.- Continued.



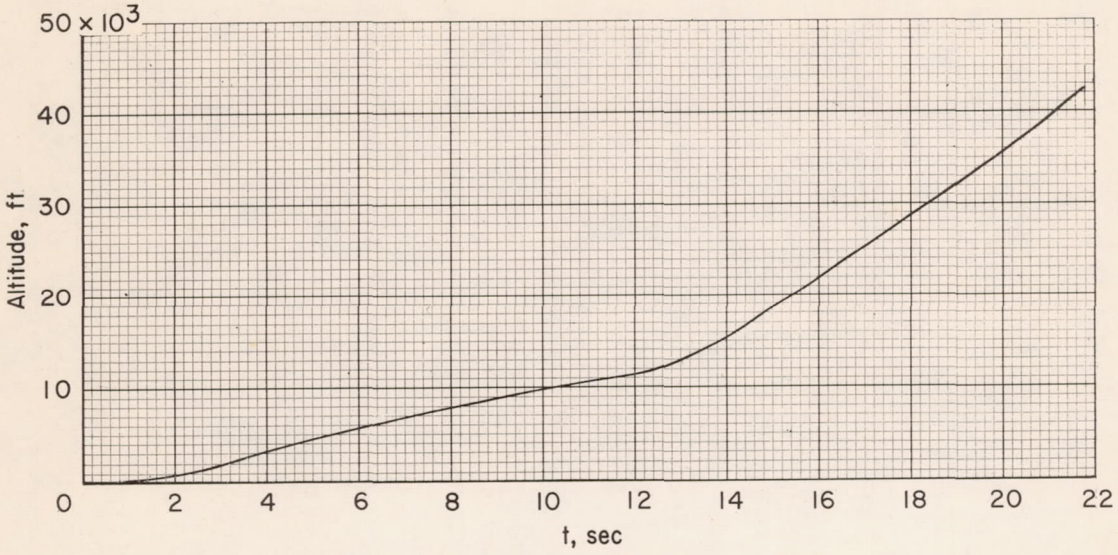
(c) Model and booster on launcher. L-86311

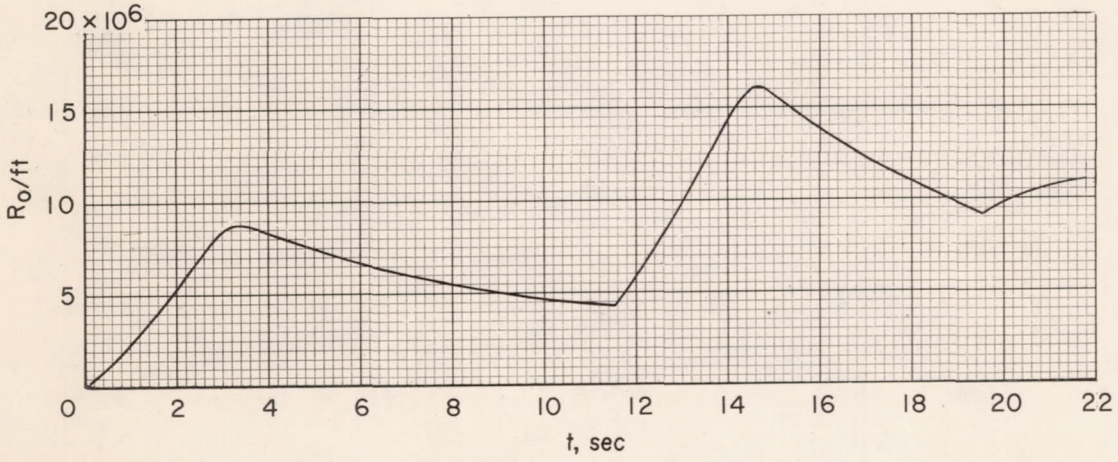
Figure 1.- Concluded.



(a) Time histories of Mach number and measured skin temperatures.

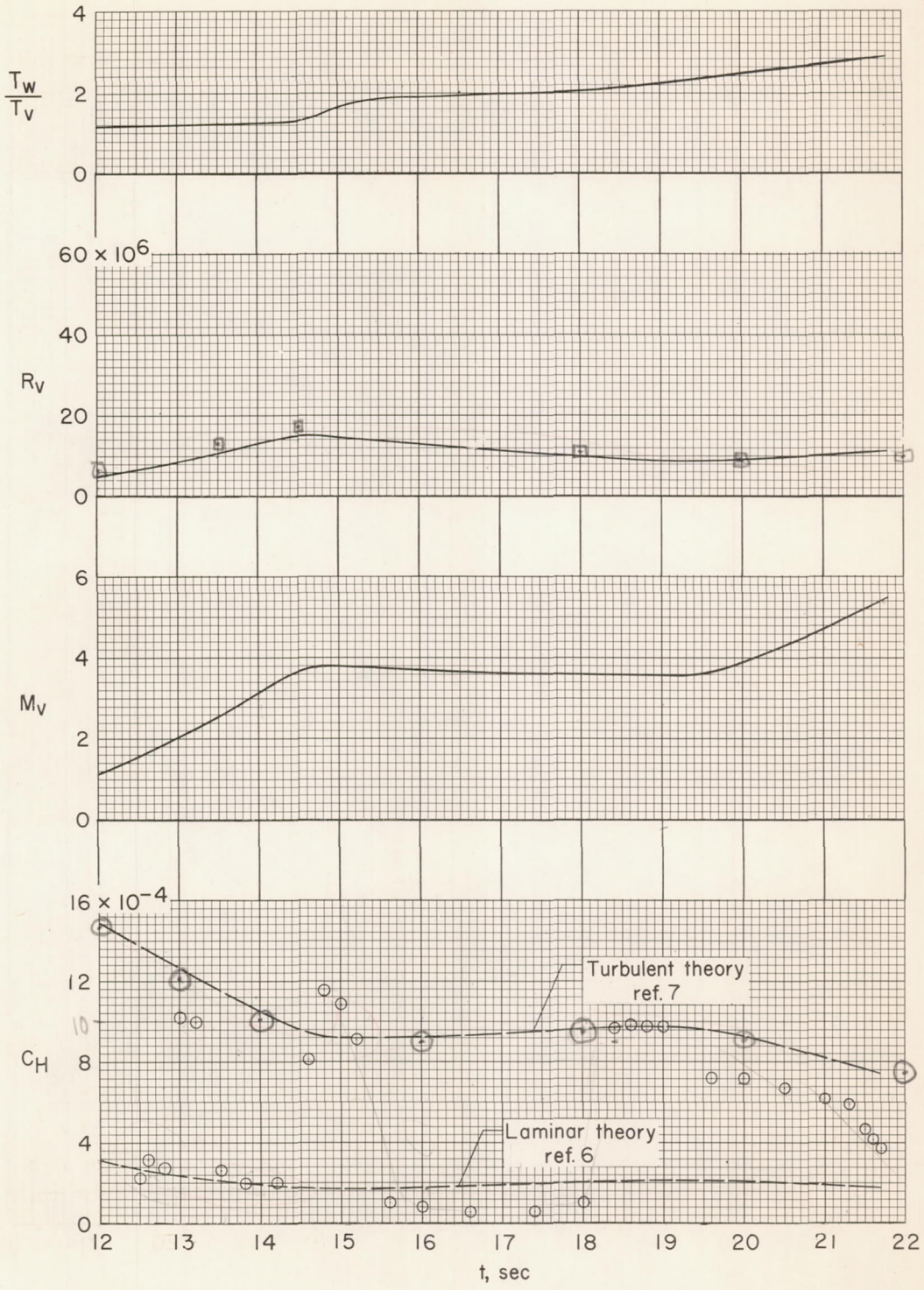
Figure 2.- Test conditions.





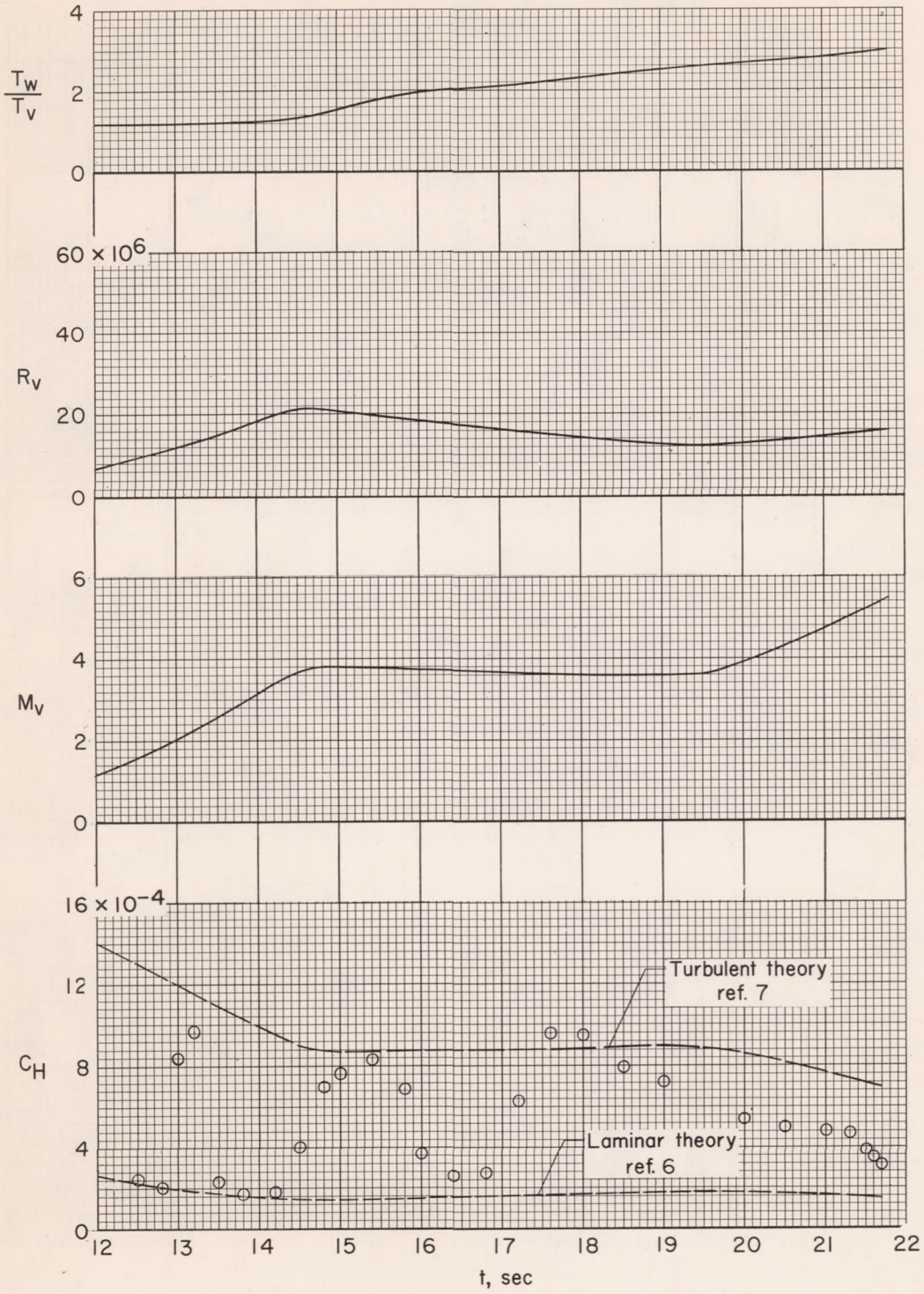
(b) Time histories of altitude and free stream Reynolds number per foot.

Figure 2.- Concluded.



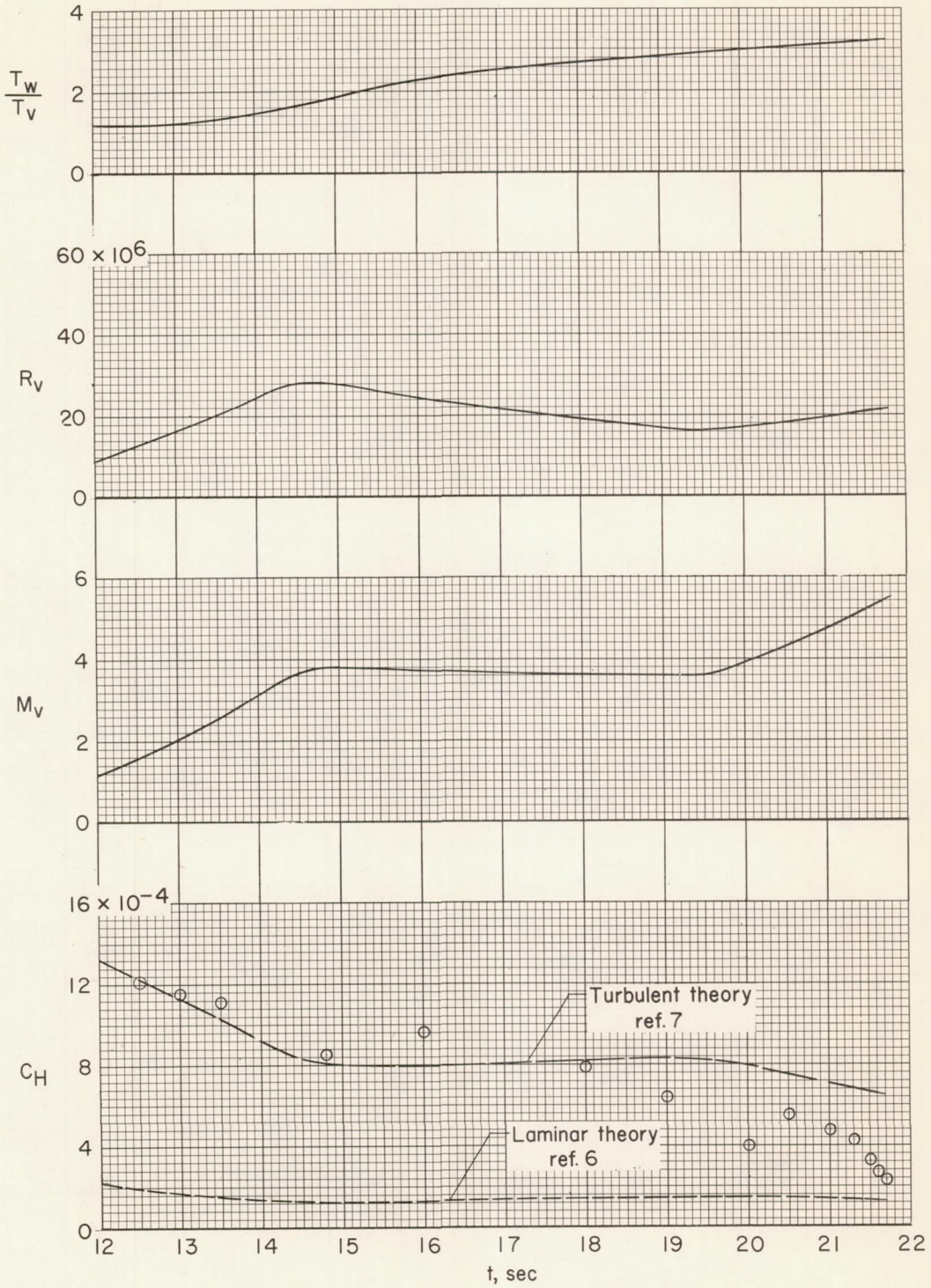
(a) Station 10.

Figure 3.- Time histories of heat-transfer coefficient and controlling parameters.



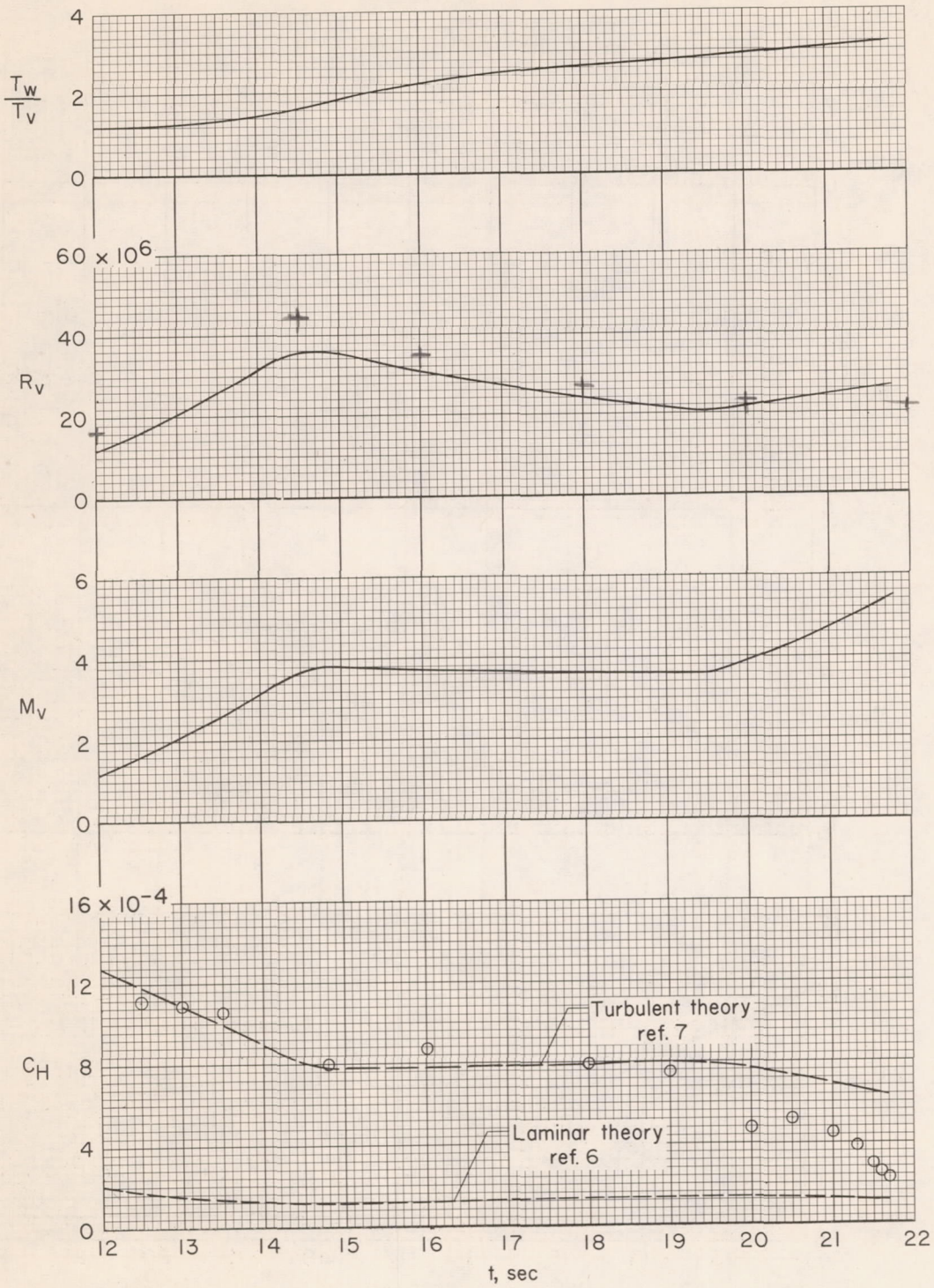
(b) Station 14.

Figure 3.- Continued.



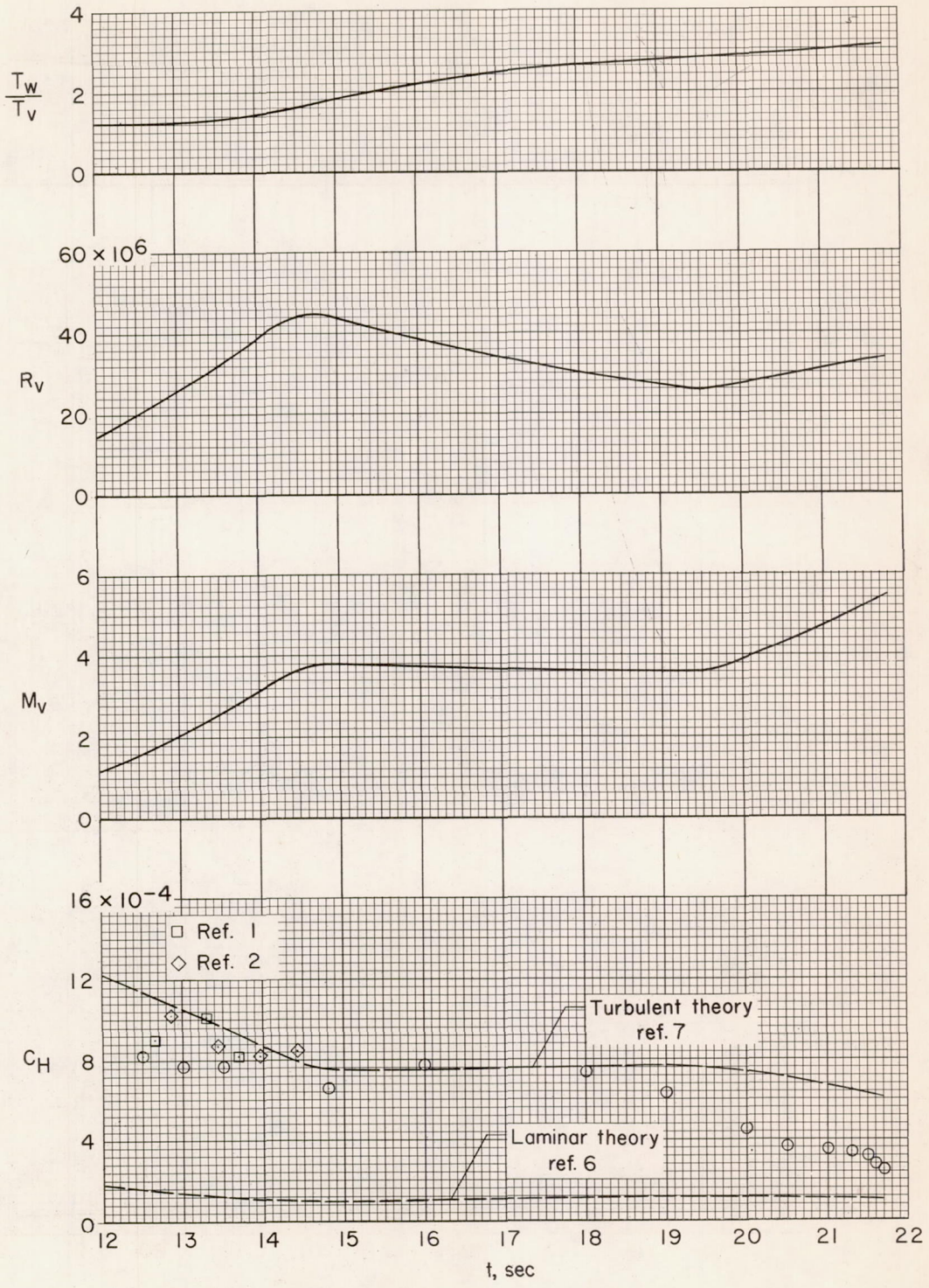
(c) Station 19.

Figure 3.- Continued.



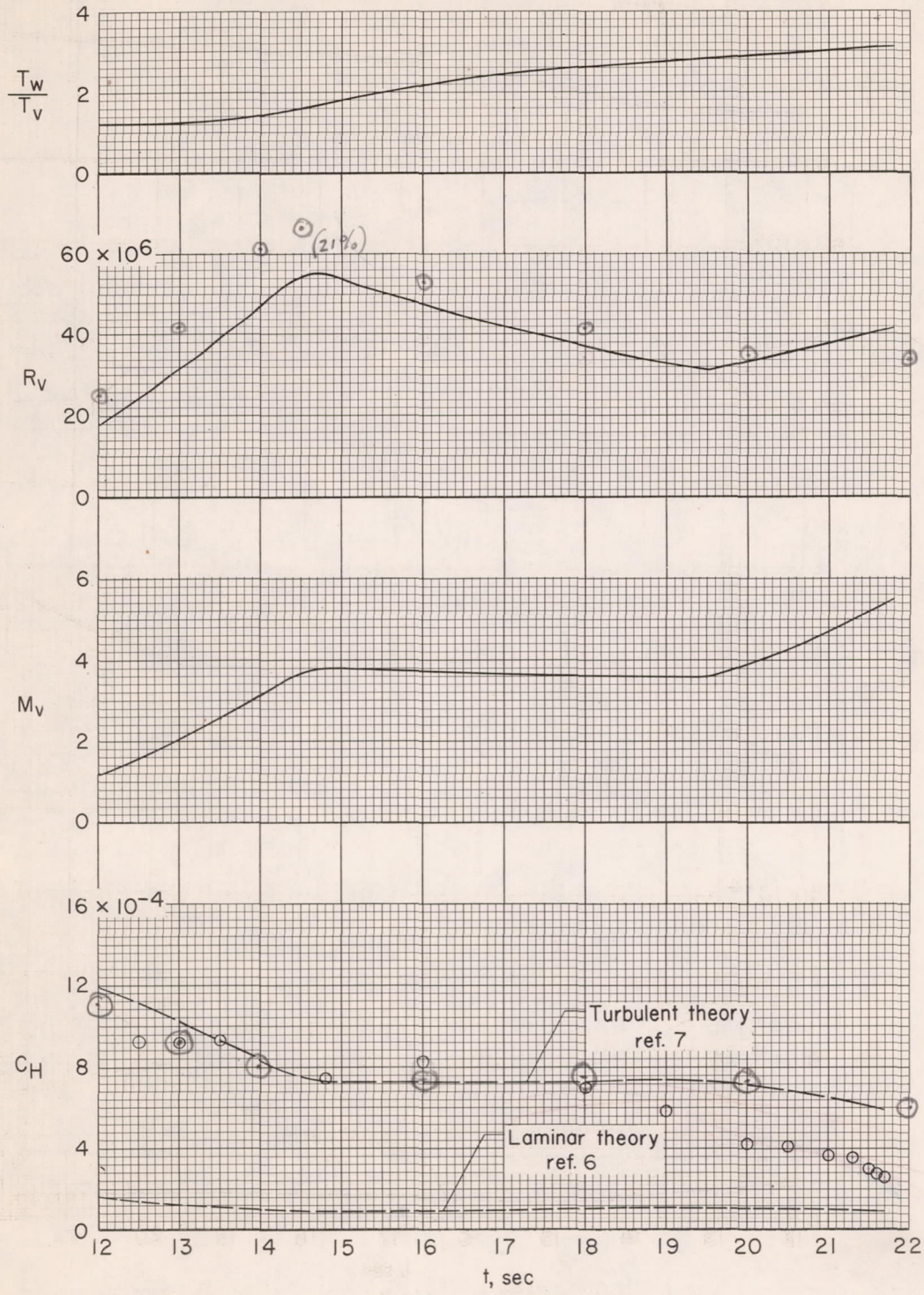
(d) Station 24.

Figure 3.- Continued.



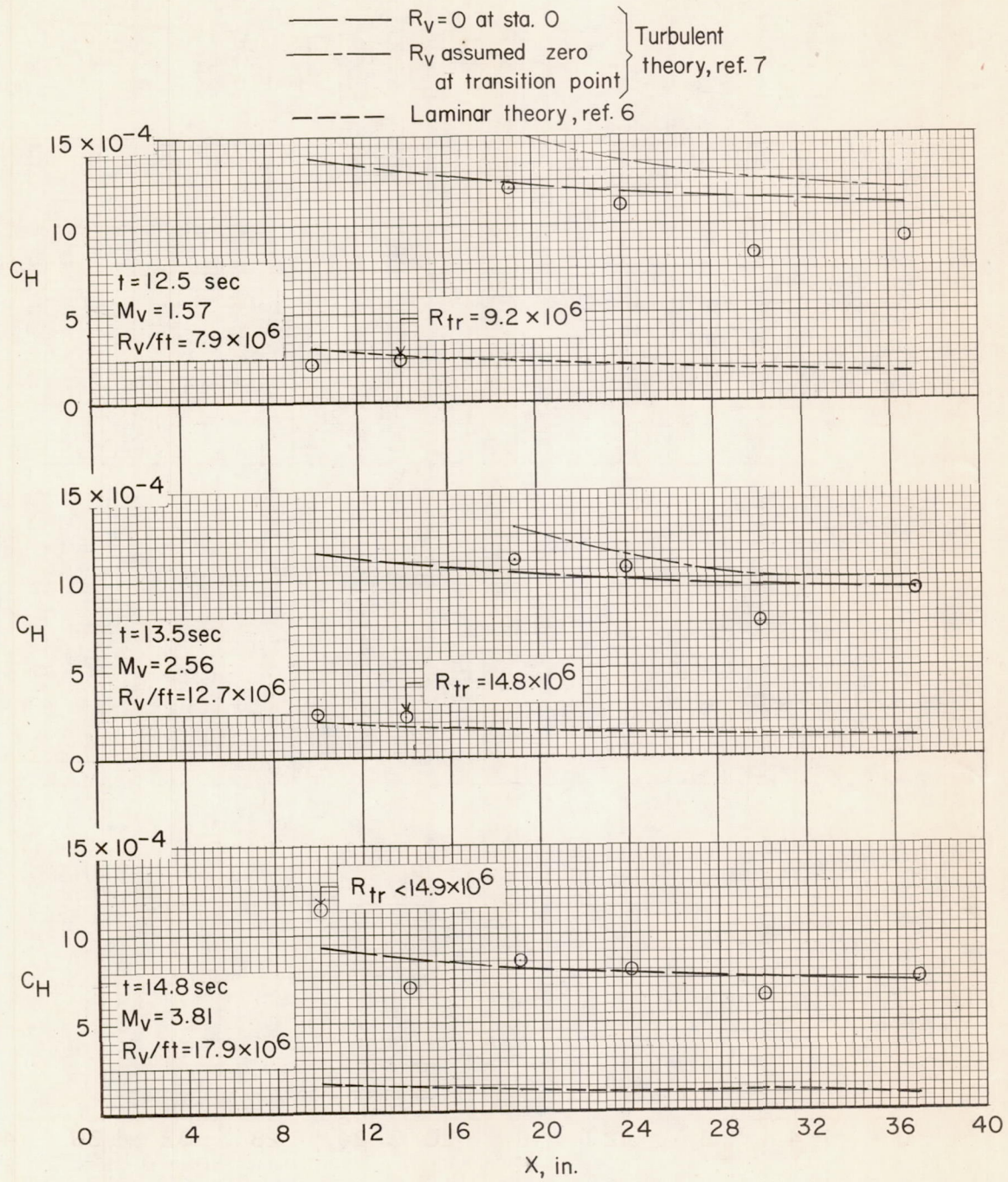
(e) Station 30.

Figure 3.- Continued.



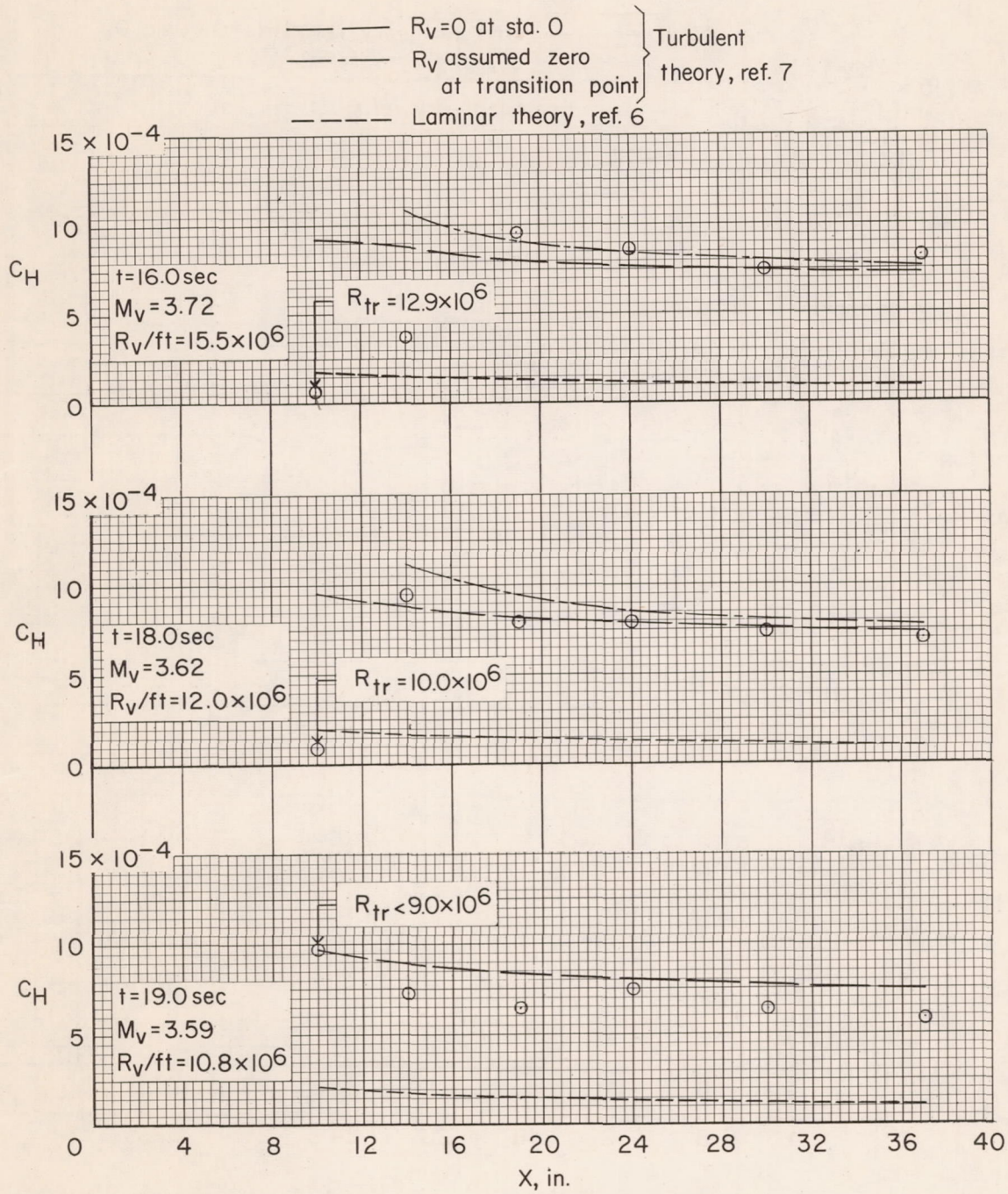
(f) Station 37.

Figure 3.- Concluded.



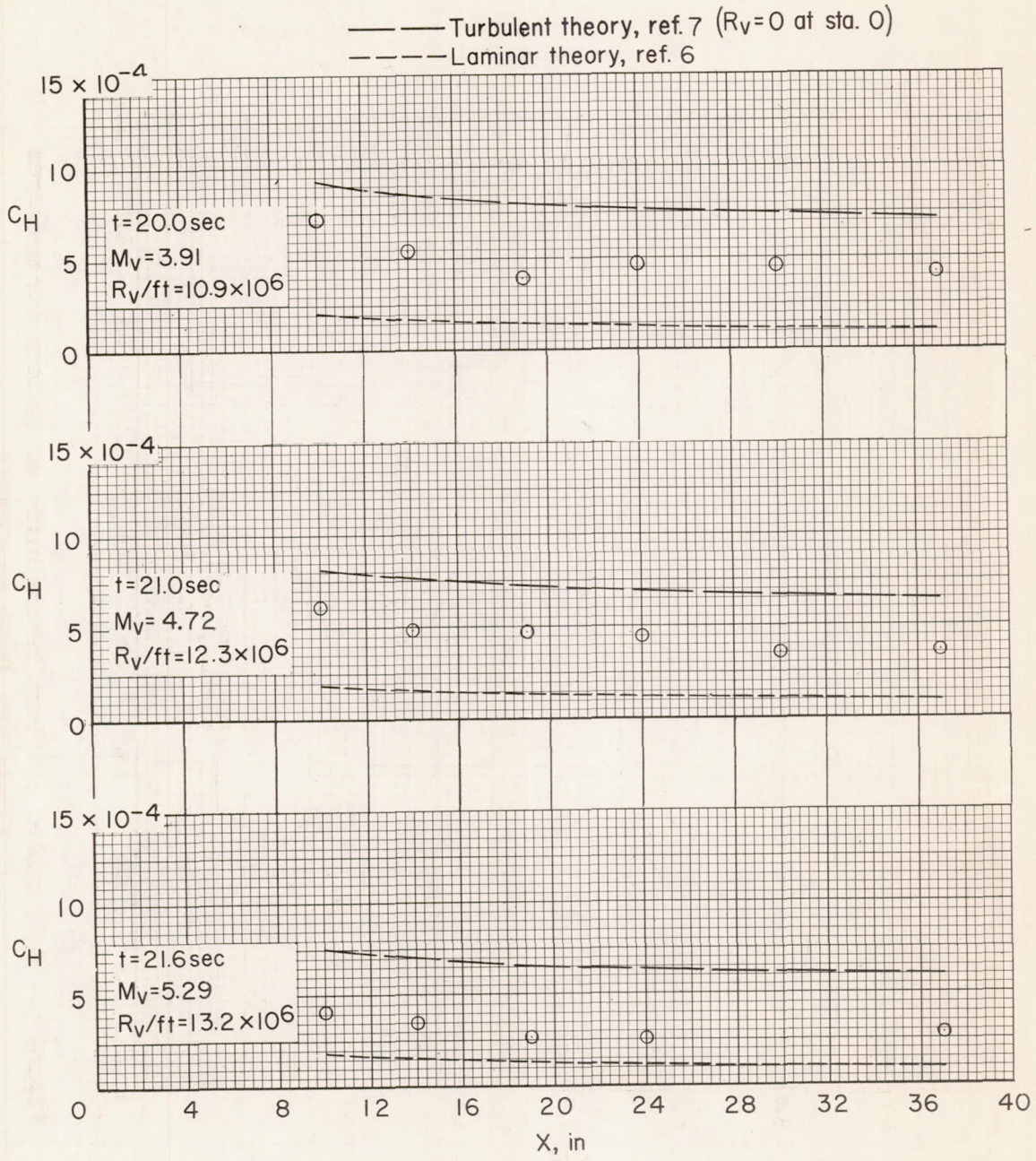
(a) Times: 12.0, 13.5, and 14.8 seconds.

Figure 4.- Variation of heat-transfer coefficient along the conical nose at several times.



(b) Times: 16.0, 18.0, and 19.0 seconds.

Figure 4.- Continued.



(c) Times: 20.0, 21.0, and 21.6 seconds.

Figure 4.- Concluded.

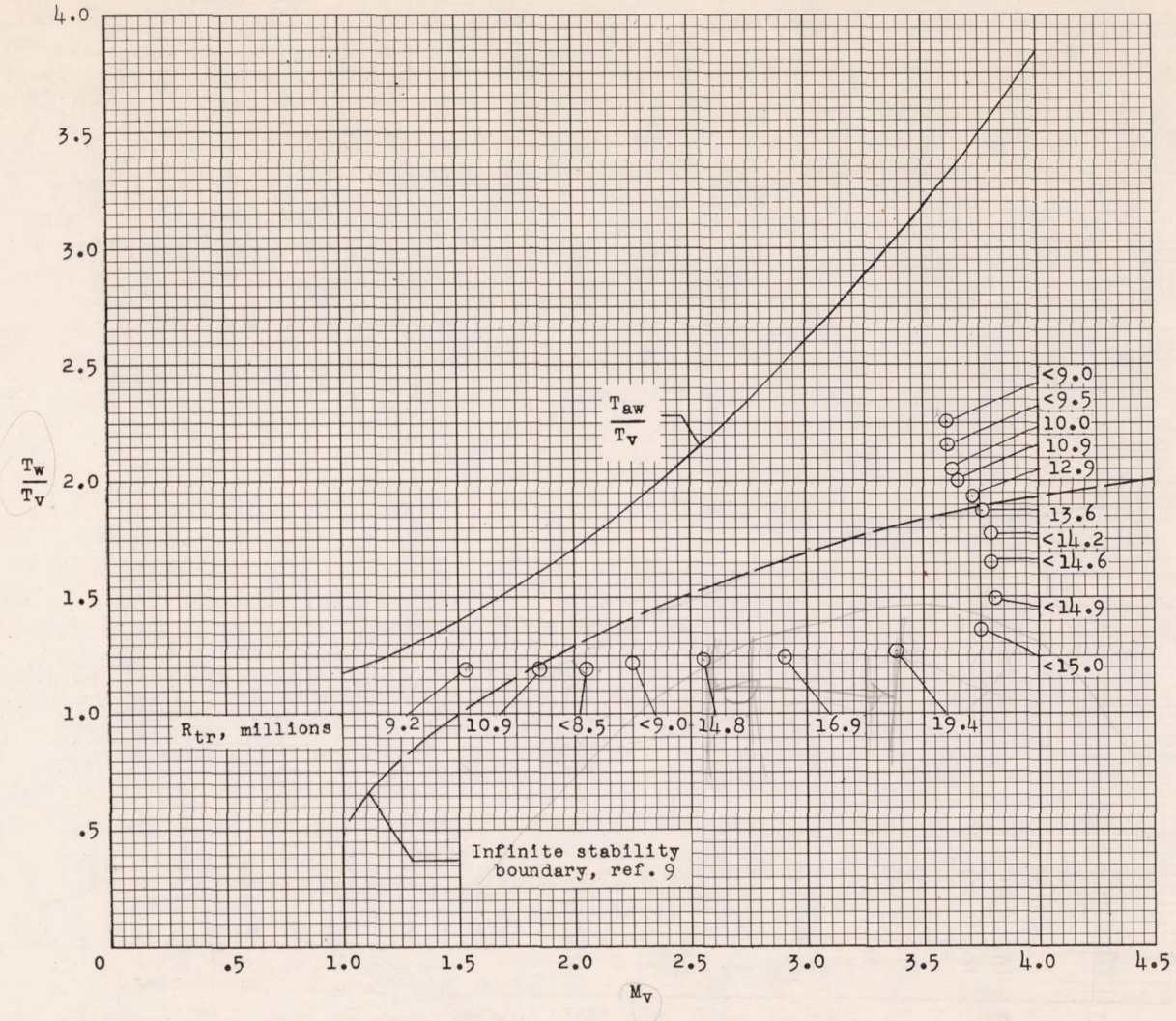
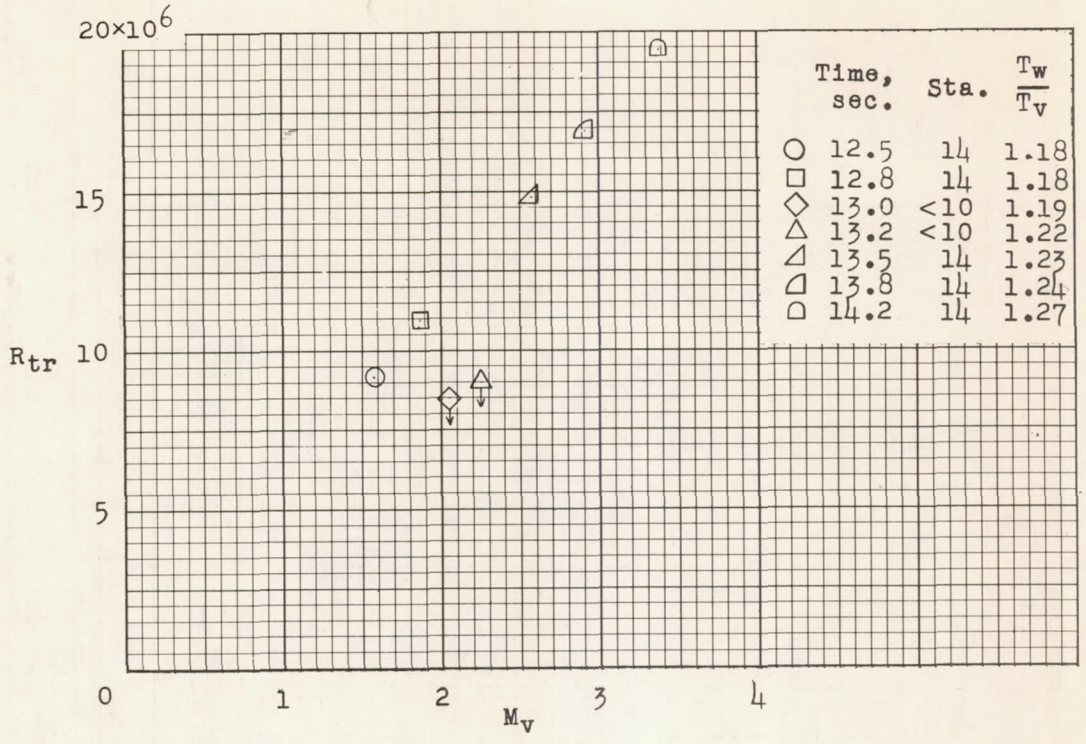
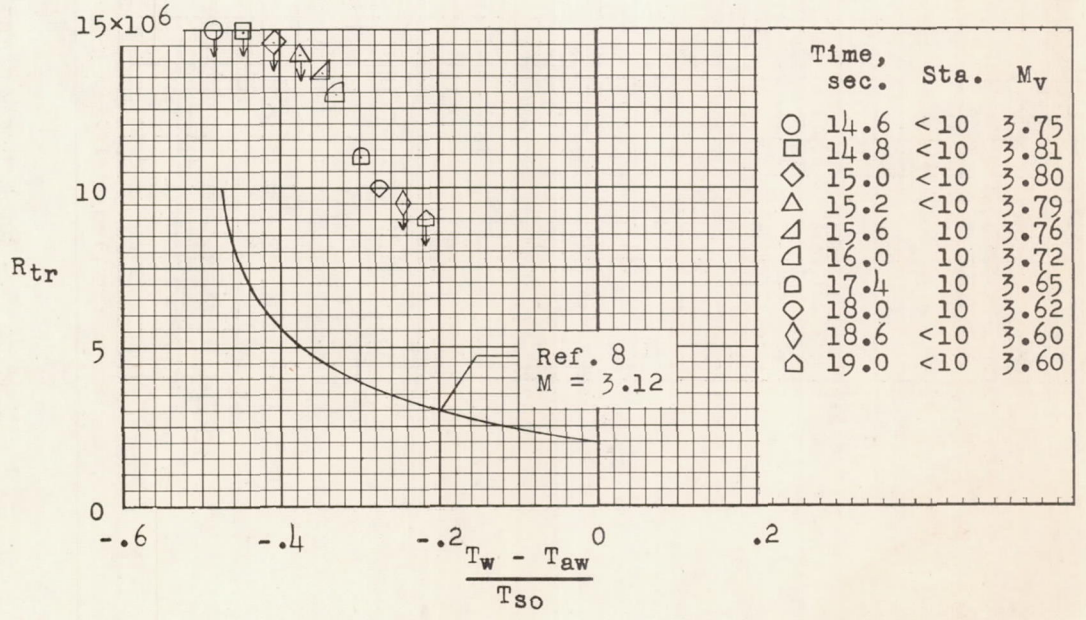


Figure 5.- Mach number and temperature ratio conditions for measured transition Reynolds numbers.



(a) Transition Reynolds numbers at a wall-to-static temperature ratio of approximately 1.2.



(b) Transition Reynolds numbers at a Mach number of approximately 3.7.

Figure 6.- Experimental transition Reynolds numbers.

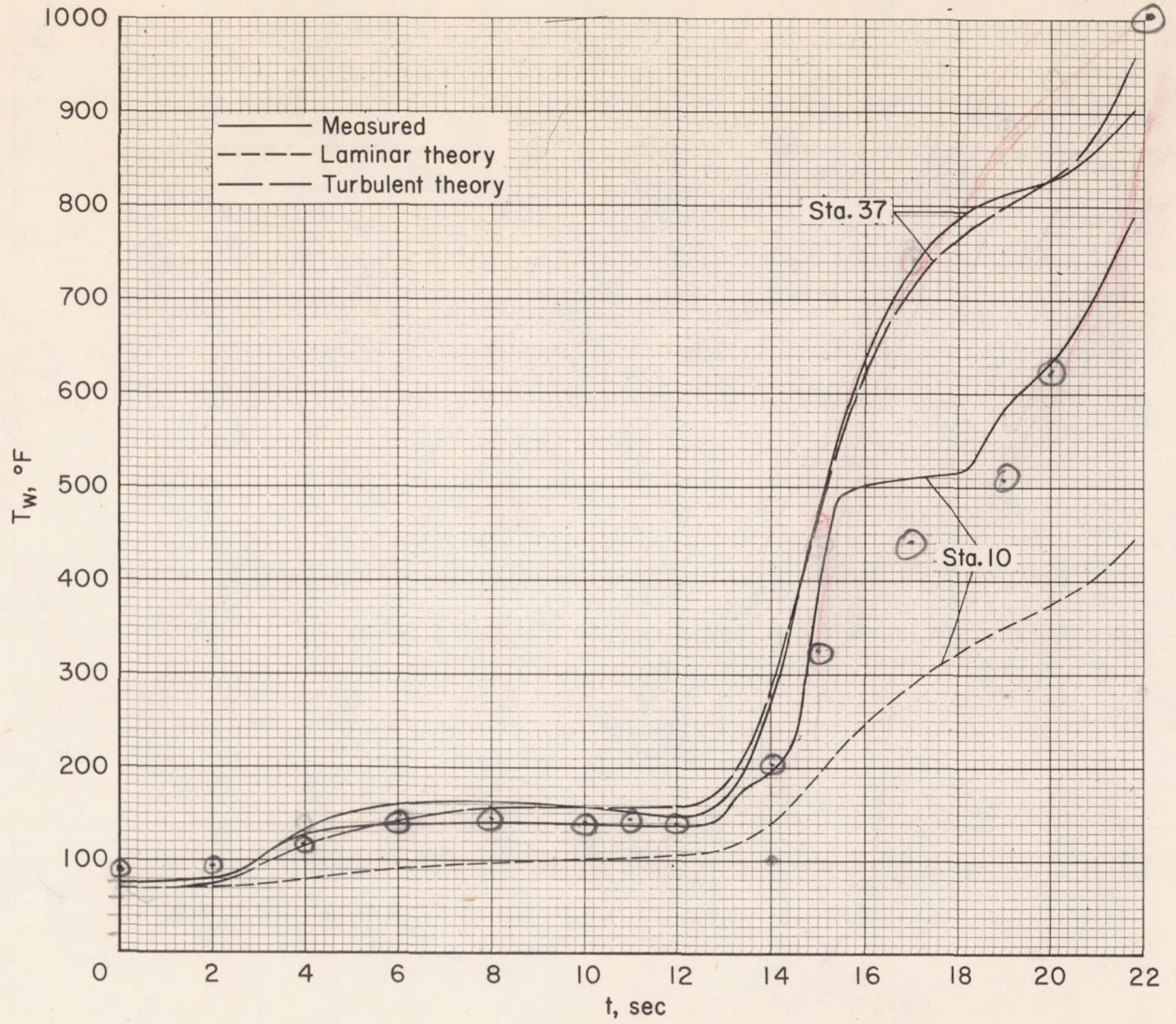


Figure 7.- Comparison of measured and computed skin temperatures.

NACA - Langley Field, Va.
CONFIDENTIAL